

# A Dynamic-Translinear Fully-Integrated Highly-Directional Hearing Aid Adapter

D. Rocha, W. A. Serdijn

Delft University of Technology  
 Mekelweg 4 - P.O. Box 5031 - 2600 GA Delft - The Netherlands  
 D.Rocha@its.tudelft.nl

## Abstract

A directional hearing aid adapter was designed and implemented using Dynamic Translinear (DTL) circuit techniques. The signal-processing core was optimized to yield minimum current consumption for the specified dynamic range. In this paper the design and implementation of the core is presented. It consumes a current of 40  $\mu\text{A}$  at a supply voltage of down to 1.0 V having a total integrated capacitance of 400 pF for a dynamic range of 50 dB.

## 1. Introduction

Hearing-impaired people have difficulties in perceiving speech in environments with considerable background noise. This is generally known as the "cocktail party" effect. Recently, directional beam-forming techniques using microphone arrays have been proposed as a solution for considerably improving speech intelligibility in crowded environments [8]. Prototypes have successfully been tested on patients and expectations are high. However, aesthetics and usability are of prime importance for successful market implantation. In practical terms, this means that the product should be invisible to the naked eye and consume as low a current as possible, being ideally self-sustaining.

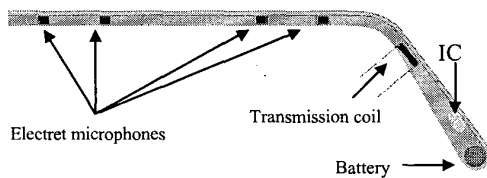


Figure 1. Proposed prototype of the directional hearing aid adapter (courtesy of Microtronic)

A first prototype, mounted on the feather of a normal pair of spectacles, as shown in Figure 1, has been designed and implemented. It consists of four non-equidistantly placed, omnidirectional electret microphones, an IC, a transmission coil, an on/off switch and a battery. The acoustic signal is picked up via the microphones and fed to the signal-processing IC, which generates a directional version of the acoustic field and feeds it electromagnetically via a high-inductance transmission coil to a standard hearing aid with pickup coil on T-position. The whole system is fed by a 1.3 V zinc-air battery and has a switch to

selectively turn it on and off. In this paper, we shall present the design and implementation of the signal-processing IC.

## 2. The PGP concept

Recently, a technique to achieve high directivity at all frequencies using as little as possible omnidirectional microphones and realizable in analogue electronics has been proposed (Figure 2)[1][2]. The core of this system is formed by the so-called Pressure-Gradient-Processors (PGP), whose block diagram is depicted in Figure 3.

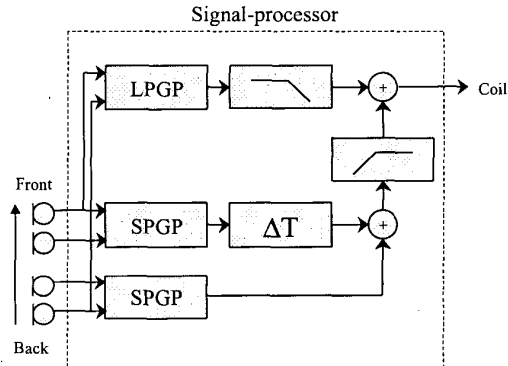


Figure 2. Block diagram of the signal processor using the PGP concept

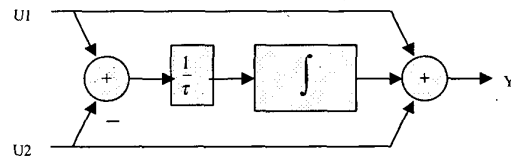
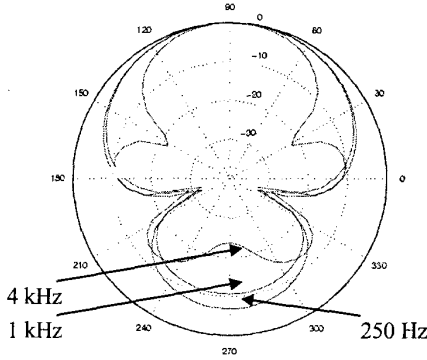


Figure 3. Block diagram of the Pressure Gradient Processor

The PGP calculates the pressure and the particle velocity of the sound field in the direction colinear to the microphone array to obtain directivity [1]. The Short Pressure Gradient Processors (SPGP) deliver high-frequency (1–5 kHz) directivity, while the Long Pressure Gradient Processors (LPGP) process mainly the lower frequency spectrum (100–1000 Hz), the difference lying solely in the associated time constant  $\tau$ . The resulting directivity

pattern on a two-dimensional plane is shown in **Figure 4** for several input signal frequencies. Reference [1] gives a deeper insight into the theory of beamforming methods as applied to sound fields.



**Figure 4.** Directivity patterns resulting from the PGP system. Input signal at  $f = 250$  Hz, 1 kHz, 4 kHz

### 3. State-space description

Having obtained a functional description of the system, the next step is to map this functionality onto a certain implementation. State-space techniques have proven to be very powerful tools in the design and optimization of multiple-input, multiple-output systems [3]. In this section a state-space description of the system is derived.

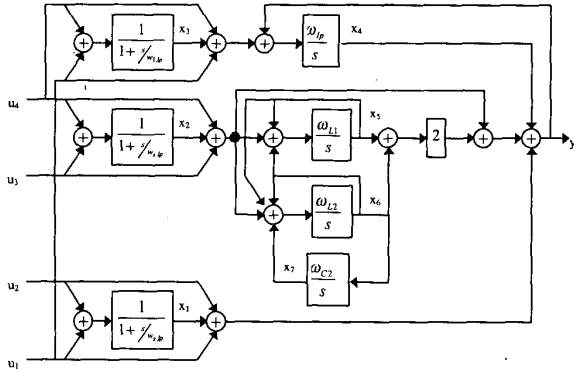


**Figure 5.** Block diagram of the implemented IC

A signal-flow graph of the designed system is given in **Figure 5**. This system has  $n_u = 4$  inputs and can be represented by  $n_x = 7$  first order differential equations.

As can be seen on the signal-flow graph, the actual implementation of the PGPs uses a lossy integrator instead of the ideally loss-less one. This is to prevent saturation of the state variables when in presence of low-frequency out-of-band input signals and offset.

Taking the outputs of the integrators as the state variables, the following state-space equations can be deduced:

$$\dot{\bar{x}} = A\bar{x} + B\bar{u} \quad (1)$$

$$y = C\bar{x} + D\bar{u}$$

$$A = \begin{pmatrix} -\omega_p & 0 & 0 & 0 & 0 & 0 & 0 \\ 0 & -\omega_p & 0 & 0 & 0 & 0 & 0 \\ 0 & 0 & -\omega_p & 0 & 0 & 0 & 0 \\ -\omega_p & \omega_p & \omega_p & -\omega_p & -2\omega_p & -2\omega_p & 0 \\ 0 & \omega_{L1} & 0 & 0 & -\omega_{L1} & -\omega_{L1} & 0 \\ 0 & \omega_{L2} & 0 & 0 & -\omega_{L2} & -\omega_{L2} & -\omega_{L2} \\ 0 & 0 & 0 & 0 & 0 & \omega_{C2} & 0 \end{pmatrix} \quad B = \begin{pmatrix} -\omega_p & \omega_p & 0 & 0 \\ 0 & -\omega_p & -\omega_p & \omega_p \\ -\omega_p & 0 & 0 & \omega_p \\ 0 & 0 & \omega_{L1} & \omega_{L1} \\ 0 & 0 & \omega_{L2} & \omega_{L2} \\ 0 & 0 & 0 & 0 \end{pmatrix}$$

$$C = (1 \ -1 \ 0 \ 1 \ 2 \ 2 \ 0)$$

$$D = (1 \ 1 \ -1 \ -1)$$

In order to facilitate accurate mapping onto a circuit implementation, equation (1) can be pre-multiplied by the diagonal matrix  $T$ , in which  $t_{ii} = 1/(\text{greatest common divisor of } \{a_{ij}, j=1..n_x\} \text{ and } \{b_{ij}, j=1..n_u\})$ , so as to transform all coefficients into rational numbers with small integer numerators and denominators. The following equation results:

$$T\dot{\bar{x}} = TA\bar{x} + TB\bar{u} \quad (2)$$

$$TA = \begin{pmatrix} -1 & 0 & 0 & 0 & 0 & 0 & 0 \\ 0 & -1 & 0 & 0 & 0 & 0 & 0 \\ 0 & 0 & -1 & 0 & 0 & 0 & 0 \\ -1 & 1 & 1 & -1 & -2 & -2 & 0 \\ 0 & 1 & 0 & 0 & -1 & -1 & 0 \\ 0 & 1 & 0 & 0 & -1 & -1 & -1 \\ 0 & 0 & 0 & 0 & 0 & 1 & 0 \end{pmatrix} \quad TB = \begin{pmatrix} -64 & 64 & 0 & 0 \\ 0 & 0 & -64 & 64 \\ -128 & 0 & 0 & 128 \\ 0 & -1 & 1 & 2 \\ 0 & 0 & 1 & 1 \\ 0 & 0 & 1 & 1 \\ 0 & 0 & 0 & 0 \end{pmatrix}$$

Scaling the state variables in order to have similar signal levels, which is beneficial from a dynamic range point of view [3], we arrive at the definitive state-space equations:

$$\Lambda^{-1}TA\Lambda = \begin{pmatrix} -1 & 0 & 0 & 0 & 0 & 0 & 0 \\ 0 & -1 & 0 & 0 & 0 & 0 & 0 \\ 0 & 0 & -1 & 0 & 0 & 0 & 0 \\ -1 & 1 & \frac{1}{2} & -1 & -2 & -\frac{1}{2} & 0 \\ 0 & 1 & 0 & 0 & -1 & -\frac{1}{2} & 0 \\ 0 & 4 & 0 & 0 & -4 & -1 & -2 \\ 0 & 0 & 0 & 0 & 0 & \frac{1}{2} & 0 \end{pmatrix} \quad \Lambda^{-1}TB = \begin{pmatrix} -64 & 64 & 0 & 0 \\ 0 & 0 & -64 & 64 \\ -192 & 0 & 0 & 192 \\ 0 & -1 & 1 & 2 \\ 0 & 0 & 1 & 1 \\ 0 & 0 & 4 & 4 \\ 0 & 0 & 0 & 0 \end{pmatrix}$$

$$C\Lambda = (1 \ -1 \ 0 \ 1 \ 2 \ \frac{1}{2} \ 0)$$

$$D = (1 \ 1 \ -1 \ -1)$$

$\Lambda$  being the diagonal scaling matrix.

### 4. Dynamic range optimization

The dynamic range of a filter is determined by the ratio of the signal level to the noise level. Taking as a reference point for our calculations the output of the filter and feeding the system with 4 non-correlated input signals with a white signal spectrum, one can easily see, that the output signal level depends only on the input signal and the input-output transfer matrix.

To estimate the dynamic range, apart from the above-mentioned output signal level, also the output noise level needs to be calculated. This noise stems from the basic building blocks that constitute the signal processor, in this case, the integrators. The translinear embodiment of a lossy integrator is depicted in **Figure 6** [6].

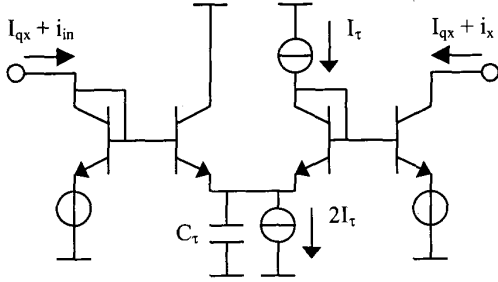


Figure 6. Possible implementation of an integrator

The major noise sources in the integrator will be the transistors' shot noise, which can be represented by two equivalent white noise sources, one at the input and one at the output of every integrator:

$$S_{n,in,i} = S_{n,out,i} = 2qI_{qx} \left(1 + \frac{I_{qx}}{I_{\tau}}\right) = 2qI_{qx} \left(1 + \frac{1}{\gamma_i}\right)$$

$\gamma_i$  represents the ratio between the integration time-constant current  $I_i$  and the quiescent state-current  $I_{qi}$ .

At this stage, it is useful to introduce an important transfer characteristics, which will be used in subsequent calculations. We shall use the matrix  $G$ , representing the transfer from the input of the integrators to the output of the system.

$$G = C(sI - A)^{-1}$$

In this equation,  $s$  represents the Laplace operator and  $I$  is the  $n_x \times n_x$  identity matrix.

Figure 7 is part of the direct representation of equation (2).

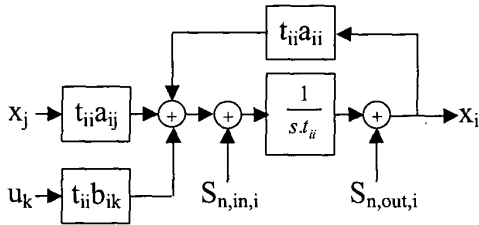


Figure 7. Detail of one integrator

The noise sources  $S_{n,in,i}$  and  $S_{n,out,i}$  presented above add noise to the input and output of integrator  $i$ , respectively.  $S_{n,out,i}$  can be transformed to the input of integrator  $i$ . The resulting noise source at the input of every integrator, thus becomes:

$$S_{n,i} = S_{n,in,i} + S_{n,out,i} |j\omega t_{ii}|^2 + \sum_{k=1}^{n_k} S_{n,u_k} |t_{ii} b_{ik}|^2$$

Considering that the noise contribution from the input can always be made sufficiently small, the noise at the output of the system can be approximately calculated as follows:

$$N_y = 2qI_{qx} \sum_{i=1}^{n_x} \left(1 + \frac{1}{\gamma_i}\right) \int_{-\omega_B}^{\omega_B} (1 + |j\omega t_{ii}|^2) |g_i(j\omega)|^2 d\omega$$

Since the state variables have previously been scaled,  $I_{qx}$ , the quiescent state variable current, has been considered equal for all integrators.  $\omega_B = 2\pi \cdot 5000$  rad.s<sup>-1</sup> represents the signal bandwidth.

Given a certain amount of available on-chip capacitance  $C$  and using the method of Lagrange multipliers [3][5], one can easily find the distribution of  $\gamma_i$ 's that will lead to the minimum amount of noise at the output:

$$C = \sum_{i=1}^{n_x} C_{\tau_i} = \frac{I_{qx}}{U_T} \sum_{i=1}^{n_x} \gamma_i t_{ii}$$

$$\gamma_k = \frac{\sqrt{m_k/t_{kk}}}{\sum_{i=1}^{n_x} \sqrt{m_i/t_{ii}}} \frac{C U_T}{I_{qx}}$$

For the sake of a convenient representation the variable  $m_i$  was introduced:

$$m_i = \int_{-\omega_B}^{\omega_B} (1 + |j\omega t_{ii}|^2) |g_i(j\omega)|^2 d\omega$$

The  $I_{qx}$  needed to reach the specified dynamic range can be calculated by solving the ratio of output signal level to output noise level for  $I_{qx}$ . The whole noise curve shifts proportionally to the quiescent current  $I_{qx}$ .

## 5. Simulation Results

The circuit was implemented in bipolar technology using the lossy integrators represented in Figure 6 as basic building blocks. In this section PStar (analogue circuit simulator from Philips) simulation results will be presented.

Table 1 represents the values of the implemented capacitors and quiescent currents.

$C_{\tau 1}$	76.5 pF
$C_{\tau 2}$	76.5 pF
$C_{\tau 3}$	94.1 pF
$C_{\tau 4}$	50.8 pF
$C_{\tau 5}$	65.6 pF
$C_{\tau 6}$	7.8 pF
$C_{\tau 7}$	28.8 pF
$I_{qx}$	200 nA
$I_{qy}$	157 nA

Table 1. Values of capacitors and quiescent currents

Figure 8 gives the amplification of the input signal as a function of the angle (in radians) of a simulated acoustic signal source for a 1kHz input signal. The ideal and actual curves are represented, the deviation stemming from the transistors' finite output resistance.

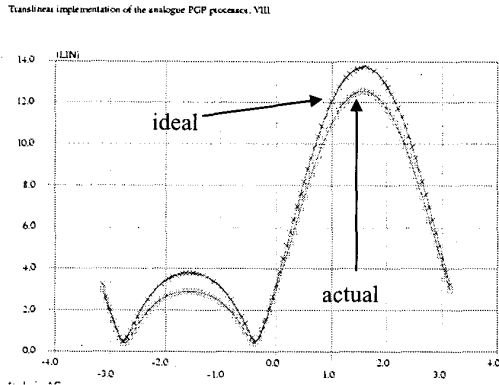


Figure 8. Output signal as a function of the angle of the acoustic signal source

The total output noise is depicted in Figure 9. Integration in the signal-band from 100 Hz to 5kHz gives the desired signal-noise ratio of 50.5 dB.

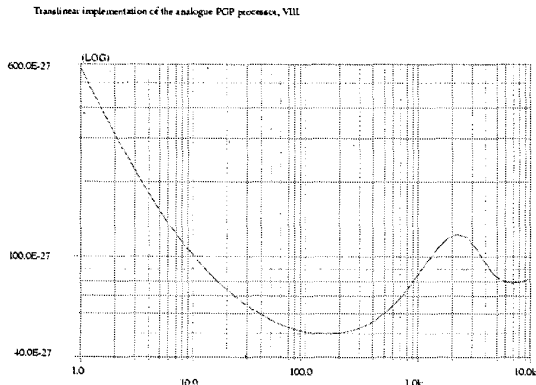


Figure 9. Total output noise

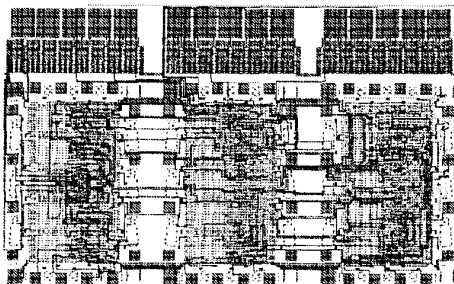


Figure 10. Chip layout

## 6. Chip layout

The signal-processing core presented above was co-integrated with 4 pre-amplifiers with automatic gain control (AGC) and an output amplifier on a semi-custom chip (Figure 10). The entire circuit occupies an area of 4.3 mm x 2.7 mm. A full-custom process would permit a significant area gain.

## 7. Conclusions

The design and implementation of a first prototype of a highly directional hearing aid adapter has been presented. The current and capacitance needed to reach the specified dynamic range have been optimized.

A self-sustaining, ultra-low power version of the system, using amorphous silicon solar cells tied to Li-ion backup batteries as an energy source, is currently being developed at our lab [7].

## 8. Acknowledgements

The authors would like to thank the people at the Department of Applied Physics for developing the signal-processing algorithms from an acoustical perspective. Also the close cooperation with the companies Microtronic and Essilor is highly appreciated.

This project was financed by the Dutch Technology foundation (STW) under the grant DEL.3943 in close cooperation with project DTN.3582.

## 9. References

- [1] I. Merks, *Binaural application of microphone arrays for improved speech intelligibility in noise*, DocVision BV, TU Delft, January 2000
- [2] M.M.Boone, I.L.D.M. Merks and A.Z. van Halteren, *Directional hearing device*, European Patent Application nr. 98204331.7-2211, Microtronic B.V. Amsterdam, December 1998
- [3] Gert Groenewold, *Optimal Dynamic Range Integrated Continuous-Time Filters* – Delft University Press – PhD thesis, 1992
- [4] G. Groenewold, *The design of high dynamic range continuous-time integrated bandpass filters* – IEEE Transactions on Circuits and Systems, vol 38:pp 838-852, August 1991
- [5] V. I. Smirnov, *A Course of Higher Mathematics* – Pergamon Press, Oxford, 1964
- [6] J. Mulder, W. A. Serdijn, A. C. van der Woerd and A. H. M. van Roermond, *Dynamic Translinear and Log-Domain Circuits* – Kluwer Academic Publishers, Boston, 1999
- [7] A.C. van der Woerd, A.H.M. Roermond, *Improvement of Hearing Aids by Strongly Directional Sound Sensing*, ICEMI'97, Conference Proceedings, pp. 474-478, 1997
- [8] W. Soede, A. J. Berkhou, F. A. Bilsen, *Development of a directional hearing instrument based on array technology*, Journal of the Acoustical Society of America, vol. 94, no 2, Part 1, pp 785-798, August 1993